

Article

On Cooling of Neutron Stars with a Stiff Equation of State Including Hyperons

Hovik Grigorian^{1,2}, Evgeni E. Kolomeitsev³ , Konstantin A. Maslov^{4,5} and Dmitry N. Voskresensky^{4,5,*}

¹ Laboratory for Information Technologies, Joint Institute for Nuclear Research, Dubna RU-141980, Russia; hovikgrigorian@gmail.com

² Faculty of Physics, Yerevan State University, Alek Manyukyan 1, Yerevan 0025, Armenia

³ Department of Physics, Matej Bel University, Tajovskeho 40, SK-97401 Banska Bystrica, Slovakia; E.Kolomeitsev@gsi.de

⁴ Bogoliubov Laboratory for Theoretical Physics, Joint Institute for Nuclear Research, Dubna RU-141980, Russia; const.maslov@gmail.com

⁵ Department of Theoretical Nuclear Physics, National Research Nuclear University (MEPhI), Kashirskoe shosse 31, Moscow RU-115409, Russia

* Correspondence: D.Voskresensky@gsi.de

Received: 29 November 2017; Accepted: 15 January 2018; Published: 8 February 2018

Abstract: Exploiting a stiff equation of state of the relativistic mean-field model MKVORH ϕ with σ -scaled hadron effective masses and couplings, including hyperons, we demonstrate that the existing neutron-star cooling data can be appropriately described within “the nuclear medium cooling scenario” under the assumption that different sources have different masses.

Keywords: neutron stars; equation of state; in-medium effects; neutrino

1. Introduction

The equation of state (EoS) of the neutron-star matter should be stiff, cf. [1,2], in order to describe measured masses of the heaviest known pulsars PSR J1614-2230 (of mass $M = 1.928 \pm 0.017M_{\odot}$) [3] and PSR J0348+0432 (of mass $M = 2.01 \pm 0.04M_{\odot}$) [4]. The presence of hyperons in neutron stars leads to a softening of the EoS which results in a decrease of the maximum neutron-star mass below the measured values of masses for PSR J1614-2230 and PSR J0348+0432 pulsars, if one exploits ordinary relativistic mean-field (RMF) models (hyperon puzzle [5,6]). However, within RMF, EoSs with σ -scaled hadron effective masses and coupling constants, the maximum neutron-star mass remains above $2M_{\odot}$ even when hyperons are included [7,8]. Additionally, other important constraints on the equation of state, e.g., the flow constraint from heavy-ion collisions [9,10] are fulfilled. We demonstrate how a satisfactory explanation of all existing observational data for the temperature–age relation is reached within the “nuclear medium cooling” scenario [11], now with the RMF EoS MKVORH ϕ with σ -scaled hadron effective masses and coupling constants, including hyperons [7,8].

2. Equation of State and Pairing Gaps

The EoS of the cold hadronic matter should:

- satisfy experimental information on properties of dilute nuclear matter;
- fulfil empirical constraints on global characteristics of atomic nuclei;
- satisfy constraints on the pressure of the nuclear matter from the description of particle transverse and elliptic flows and the K^+ production in heavy-ion collisions, cf. [9,10];
- allow for the heaviest known pulsars, i.e., PSR J1614-2230 (of mass $M = 1.928 \pm 0.017M_{\odot}$) [3] and PSR J0348+0432 (of mass $M = 2.01 \pm 0.04M_{\odot}$) [4];

- allow for an adequate description of the compact star cooling [11], most probably without direct Urca (DU) neutrino processes in the majority of the known pulsars detected in soft X rays [12];
- yield a mass–radius relation comparable with the empirical constraints including recent gravitation wave LIGO-Virgo detection [13];
- when extended to non-zero temperature T (for $T < T_c$ where T_c is the critical temperature of the deconfinement), appropriately describe supernova explosions, proto-neutron stars, and heavy-ion collision data, etc.

The most difficult task is to simultaneously satisfy the flow of heavy-ion collision and the maximum neutron-star mass constraints. To fulfil the flow constraints [9,10], a rather soft EoS of isospin-symmetric matter (ISM) is required, whereas the EoS of the beta-equilibrium matter (BEM) should be stiff in order to predict the maximum mass of a neutron star to be higher than the measured mass $M = 2.01 \pm 0.04 M_\odot$ [4] of the pulsar PSR J0348+0432, this mass being the heaviest among the known pulsars.

In standard RMF models, hyperons may already appear in neutron-star cores for $n \gtrsim (2 - 3)n_0$, which results in a decrease of the maximum neutron-star mass below the observed limit. Within the RMF models with the σ field-dependent hadron effective masses and coupling constants, the hyperon puzzle is resolved, see [7,8]. Here, we use the MKVOR-based models from these works. Most other constraints on the EoS, including the flow constraints, are also appropriately satisfied. In Figure 1, we demonstrate the neutron-star mass as a function of the central density for the MKVOR model without hyperons and for the MKVORH ϕ model which includes hyperons, cf. Figures 20 and 25 in [8]. For the MKVOR model, the maximum neutron-star mass reaches $2.33 M_\odot$ and the DU reaction is allowed for $M > 2.14 M_\odot$. For the MKVORH ϕ model, the maximum neutron-star mass is $2.22 M_\odot$. The DU reactions on Λ hyperons $\Lambda \rightarrow p + e + \bar{\nu}$, $p + e \rightarrow \Lambda + \nu$, become allowed for $M > 1.43 M_\odot$. The DU reactions with participation of Ξ^- , $\Xi^- \rightarrow \Lambda + e + \bar{\nu}$ and $\Lambda + e \rightarrow \Xi^- + \bar{\nu}$ become allowed for $M > 1.65 M_\odot$. The neutrino emissivity in these processes is typically smaller than that in the standard DU processes on nucleons due to a smaller coupling constant for the hyperons (cf. 0.0394 factor for the DU process $\Lambda \rightarrow p + e + \bar{\nu}$ and 0.0175 for $\Xi^- \rightarrow \Lambda + e + \bar{\nu}$ compared to 1 for the DU process on nucleons). Besides, we should bear in mind that the pairing suppression R -factors for the DU processes on nucleons and hyperons are different and in our model, for the EoS in the region in which there are hyperons, the R -factor for DU processes on nucleons is larger than that on hyperons.

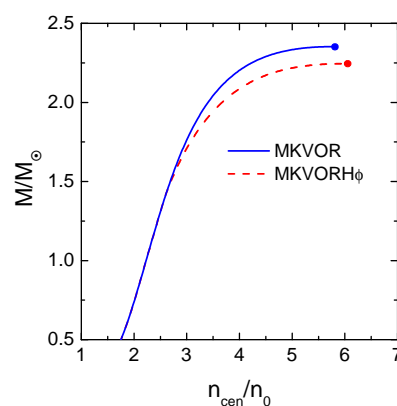


Figure 1. Neutron-star masses versus the central density for the MKVOR model without the inclusion of hyperons and for the MKVORH ϕ model with hyperons included.

We adopt here all cooling inputs such as the neutrino emissivities, specific heat, crust properties, etc., from our earlier works performed on the basis of the HHJ equation of state (EoS) [11,14,15], a stiffer HDD EoS [16] and even stiffer DD2 and DD2vex EoSs [17] for the hadronic matter. These works exploit the nuclear medium cooling scenario, where the most efficient processes are the medium-modified

Urca (MMU) processes, $nn \rightarrow npe\bar{\nu}$ and $np \rightarrow ppe\bar{\nu}$, medium-modified nucleon bremsstrahlung (MNB) processes $nn \rightarrow nn\nu\bar{\nu}$, $np \rightarrow np\nu\bar{\nu}$, $pp \rightarrow pp\nu\bar{\nu}$, and the pair-breaking-formation (PBF) processes $n \rightarrow n\nu\bar{\nu}$ and $p \rightarrow p\nu\bar{\nu}$. The latter processes are allowed only in superfluid matter.

The results are rather insensitive to the value of the nn pairing gap since the 1S_0 neutron pairing does not spread in the interior region of the neutron star. We use the same values as we have used in our previous works, e.g., see Figure 5 in [11] for details. Within our scenario, we continue to exploit the assumption that the value of the 3P_2 nn pairing gap is tiny and its actual value does not affect the calculations of the neutrino emissivity [14]. For calculation of the proton pairing gaps, we use the same models as in [17] but now we exploit EoSs of the MKVORH ϕ model. The corresponding gaps are shown on the left panel in Figure 2.

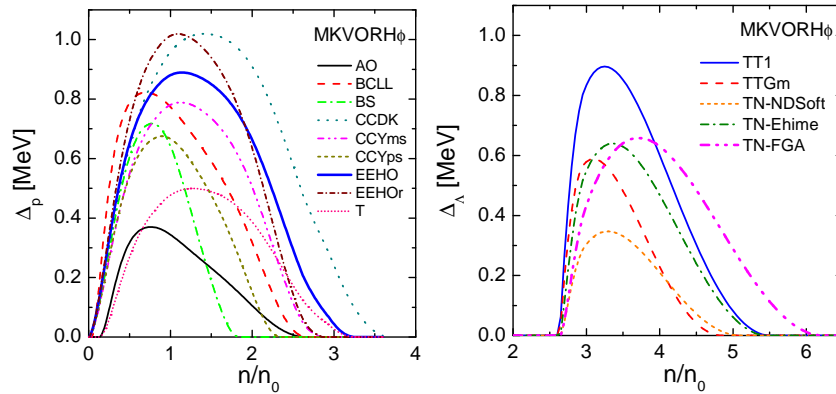


Figure 2. Pairing gaps for protons (left panel) and Λ hyperons (right panel) as functions of baryon density for the MKVORH ϕ EoS including hyperons. Proton gaps are evaluated using the same models as in [17] and the Λ hyperon gaps are from [18,19].

With the increase of the density in the MKVORH ϕ model, the Λ hyperons are the first to appear at the density $n_c^{(\Lambda)} = 2.63n_0$, and then the Ξ^- hyperons appear at $n_c^{(\Xi^-)} = 2.93n_0$. We take the values of the Λ gaps from the calculations [18,19]. The model TT1 uses the ND-soft model by the Nijmegen group for bare $\Lambda\Lambda$ interaction and model TTGm uses the results of G-matrix calculations by Lansky and Yamamoto [20] at density $2.5n_0$. The other three models include three nucleon forces and TNI6u forces for several $\Lambda\Lambda$ pairing potentials: ND-Soft, Ehime and FG-A. In the right panel, we show the Λ hyperon pairing gaps, which we exploit in this work. Ξ^- are considered unpaired.

The quantity

$$-G_{\pi}^{R-1}(\mu_{\pi}, k, n) = \omega^{*2}(k) = k^2 + m_{\pi}^2 - \mu_{\pi}^2 + \text{Re}\Sigma_{\pi}(\mu_{\pi}, k, n) \quad (1)$$

in dense neutron-star matter (for $n \gtrsim n_0$) has a minimum for $k = k_m \simeq p_F$, where p_F is the neutron Fermi momentum. For π^0 , the minimum occurs for $\mu_{\pi} = 0$. The value $\omega^{*2}(k_m)$ has the meaning of the squared effective pion gap. It enters the NN interaction amplitude and the emissivity of the MMU and MNB processes, instead of the quantity $m_{\pi}^2 + p_F^2$ entering the calculation of the NN interaction amplitude and the emissivity of the modified Urca (MU) and nucleon bremsstrahlung (NB) processes in the minimal cooling scheme. The inequality $\omega^{*2}(k_m) < m_{\pi}^2 + p_F^2$ demonstrates the effect of the pion softening. Of key importance is the fact that here we use the very same density dependence of the effective pion gap $\omega^*(n)$ as in our previous works, e.g., see Figure 2 of [17]. To be specific, we assume a saturation of the pion softening and absence of the pion condensation for $n > n_c$. We plot this pion gap in Figure 3.

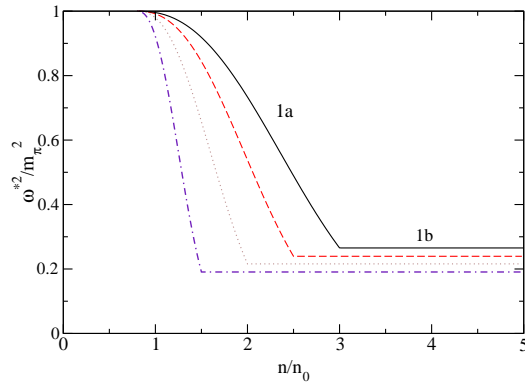


Figure 3. Density dependence of the squared effective pion gap used in the given work. We assume that the pion softening effect saturates above a critical density, the value of which we vary from 1.5 to $3n_0$.

3. Results

In the left panel in Figure 4, we show the cooling history of neutron stars calculated using the EoS of the MKVOR model without inclusion of hyperons. The demonstrated calculations employ the proton gap following the EEHO_r model shown in Figure 2, and the dotted curve in Figure 3 was used for the effective pion gap.

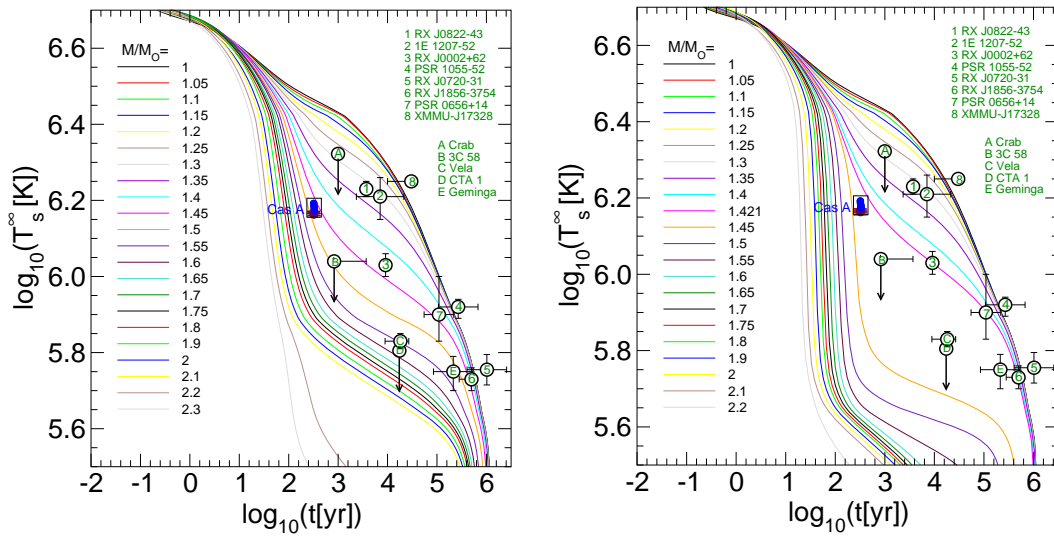


Figure 4. Redshifted surface temperature as a function of the neutron-star age for various neutron-star masses and choice of the EoS. Left panel: MKVOR model without the inclusion of hyperons. Right panel: MKVORH ϕ model with hyperons included with the gaps following from the TN-FGA parameter choice. Proton gaps for both calculations, without and with hyperons, are taken following the EEHO_r model.

In the right panel in Figure 4, we show the cooling history of neutron stars calculated using the EoS of the MKVORH ϕ model with the inclusion of hyperons. As shown in the left panel, the proton gap is given by the EEHO_r model and the effective pion gap is given by the dotted curve in Figure 3. Hyperons are taken following the TN-FGA parameter choice. We see a rather appropriate description of the data. With the given model, the DU reactions on hyperons are responsible for the cooling of the intermediate and rapid coolers (objects Cas A, B, 3, C, D, E).

With the pion gaps given by the solid and dashed curves and with proton gaps following the EEHO, EEHO_r, CCDK, CCYm, and T curves, we may also rather appropriately describe the cooling history of neutron stars within our scenario. Finally, we should mention that the effect of hyperons on

the cooling of neutron stars could be diminished, if for some reasons the hyperon pairing gaps had larger values compared to those shown in Figure 2 and would spread to a higher density. These results will be shown in our subsequent publication.

4. Conclusions

In this study, we have demonstrated that the presently known cooling data can be appropriately described within our nuclear medium cooling scenario under the assumption that different sources have different masses, provided we use the EoS of the MKVORH ϕ model (with hyperons included) at appropriately selected proton and hyperon pairing gaps.

Acknowledgments: The research was supported by the Ministry of Education and Science of the Russian Federation within the state assignment, project No 3.6062.2017/BY. The work was also supported by Slovak grant VEGA-1/0348/18. We also acknowledge the support of the Russian Science Foundation, project No 17-12-01427.

Author Contributions: All authors contributed equally to the formulation of the model, numerical analysis and writing of the paper.

Conflicts of Interest: The authors declare no conflict of interest.

References

1. Gandolfi, S.; Gezerlis, A.; Carlson, J. Neutron Matter from Low to High Density. *Ann. Rev. Nucl. Part. Sci.* **2015**, *65*, 303–328.
2. Lattimer, J.; Prakash, M. The Equation of State of Hot, Dense Matter and Neutron Stars. *Phys. Rep.* **2016**, *621*, 127–164.
3. Fonseca, E.; Pennucci, T.T.; Ellis, J.A.; Stairs, I.H.; Nice, D.J.; Ransom, S.M.; Demorest, P.B.; Arzoumanian, Z.; Crowter, K.; Dolch, T.; et al. The NANOGrav nine-year data set: Mass and geometric measurements of binary millisecond Pulsars. *Astrophys. J.* **2016**, *832*, 167.
4. Antoniadis, J.; Freire, P.C.C.; Wex, N.; Tauris, T.M.; Lynch, R.S.; van Kerkwijk, M.H.; Kramer, M.; Bassa, C.; Dhillon, V.S.; Driebe, T.; et al. A massive pulsar in a compact relativistic binary. *Science* **2013**, *340*, 448A.
5. Schaffner-Bielich, J. Hypernuclear physics for neutron stars. *Nucl. Phys. A* **2008**, *804*, 309–321.
6. Djapo, H.; Schaefer, B.; Wambach, J. On the appearance of hyperons in neutron stars. *Phys. Rev. C* **2010**, *81*, 035803.
7. Maslov, K.A.; Kolomeitsev, E.E.; Voskresensky, D.N. Solution of the hyperon puzzle within a relativistic mean-field model. *Phys. Lett. B* **2015**, *748*, 369–375.
8. Maslov, K.A.; Kolomeitsev, E.E.; Voskresensky, D.N. Relativistic mean-field models with scaled hadron masses and couplings: Hyperons and maximum neutron star mass. *Nucl. Phys. A* **2016**, *950*, 64–109.
9. Danielewicz, P.; Lacey, R.; Lynch, W. Determination of the equation of state of dense matter. *Science* **2002**, *298*, 1592–1596.
10. Lynch, W.; Tsang, M.; Zhang, Y.; Danielewicz, P.; Famiano, M.; Li, Z.; Steiner, A. Probing the symmetry energy with heavy ions. *Prog. Part. Nucl. Phys.* **2009**, *62*, 427–432.
11. Blaschke, D.; Grigorian, H.; Voskresensky, D.N. Cooling of neutron stars: Hadronic model. *Astron. Astrophys.* **2004**, *424*, 979–992.
12. Klahn, T.; Blaschke, D.; Typel, S.; van Dalen, E.N.E.; Faessler, A.; Fuchs, C.; Gaitanos, T.; Grigorian, H.; Ho, A.; Kolomeitsev, E.E.; et al. Constraints on the high-density nuclear equation of state from the phenomenology of compact stars and heavy-ion collisions. *Phys. Rev.* **2006**, *74*, 035802.
13. Abbott, B.P. LIGO Scientific and Virgo Collaborations. GW170817: Observation of gravitational waves from a binary neutron star inspiral. *Phys. Rev. Lett.* **2017**, *119*, 161101.
14. Grigorian, H.; Voskresensky, D.N. Medium effects in cooling of neutron stars and 3P(2) neutron gap. *Astron. Astrophys.* **2005**, *444*, 913–929.
15. Blaschke, D.; Grigorian, H.; Voskresensky, D.N.; Weber, F. On the cooling of the neutron star in Cassiopeia A. *Phys. Rev. C* **2012**, *85*, 022802.
16. Blaschke, D.; Grigorian, H.; Voskresensky, D.N. Nuclear medium cooling scenario in the light of new Cas A cooling data and the $2M_{\odot}$ pulsar mass measurements. *Phys. Rev. C* **2013**, *88*, 065805.

17. Grigorian, H.; Voskresensky, D.N.; Blaschke, D. Influence of the stiffness of the equation of state and in-medium effects on the cooling of compact stars. *Eur. Phys. J. A* **2016**, *52*, 67.
18. Takatsuka, T.; Tamagaki, R. Λ hyperon superfluidity in neutron star cores. *Nucl. Phys. A* **2000**, *670*, 222c.
19. Takatsuka, T.; Nishizaki, S.; Yamamoto, Y.; Tamagaki, R. Occurrence of hyperon superfluidity in neutron star cores. *Prog. Theor. Phys.* **2006**, *115*, 355–379.
20. Lansky, D.E.; Yamamoto, Y. Skyrme-Hartree-Fock treatment of Λ and $\Lambda\Lambda$ hypernuclei with G -matrix motivated interactions. *Phys. Rev. C* **1997**, *55*, 2330.



© 2018 by the authors. Licensee MDPI, Basel, Switzerland. This article is an open access article distributed under the terms and conditions of the Creative Commons Attribution (CC BY) license (<http://creativecommons.org/licenses/by/4.0/>).